Journal of Fluorescence, Vol. 15, No. 3, May 2005 (© 2005)
DOI: 10.1007/s10895-005-2636-x

Comparison of Two Tricarbocyanine-Based Dyes for Fluorescence Optical Imaging

Christin Perlitz,[1,5] Kai Licha,[1] Frank-Detlef Scholle,[1] Bernd Ebert,[2] Malte Bahner,[3] Peter Hauff,[1] Kurt Thomas Moesta,[4] and Michael Schirner[1]

Received Feburuary 17, 2005; accepted December 22, 2004

Optical technologies are evolving in many biomedical areas including the biomedical imaging disciplines. Regarding the absorption properties of physiological molecules in living tissue, the optical window ranging from 700 to 900 nm allows to use fluorescent dyes for novel diagnostic solutions. Here we investigate the potential of two different carbocyanine-based dyes fluorescent in the near infrared as contrast agents for *in vivo imaging* of subcutaneously grown tumours in laboratory animals. The primary aim was to modify the physicochemical properties of the previously synthesized dye SIDAG to investigate the effect on the *in vivo imaging* properties.

KEY WORDS: Optical imaging; NIR-dyes; contrast agents; *in vivo* imaging; tumour detection.

INTRODUCTION

Novel concepts of molecular imaging on the basis of optical technologies have been introduced rapidly during recent years. The design and application of exogenously administered fluorescent probes has allowed basic researchers and physicians to gain insight into fundamental molecular processes at the molecular, cellular, tissue and organ level. Likewise, novel biooptical technologies allowed a hand-in-hand evolution of integrated methods for the evaluation of molecular pathways and the translation of drug discovery processes into clinical benefit.

Until today two optical imaging technologies with a non-invasive approach exist in the laboratory setting for small animals, but are not established for the human patient yet [1]. That is on one hand diffuse optical tomographic (3D) imaging and on the other hand fluorescence (2D) imaging in reflection or transmission geometry. Whereas diffuse optical tomography in transmission geometry can be applied to investigate up to about 10 cm thick tissue, fluorescence reflectance imaging reaches only penetration depths up to 5 cm [2, 3].

A possible benefit for the human patient could arise from optical mammography as a tomographic approach, leading to an earlier detection of breast cancer and/or the differentiation of different forms of breast lesions. Here, during the last years considerable improvements in equipment technology have been achieved using mainly transmission geometry and advanced image algorithms for analysis [4–8]. When investigating deeper regions of tissue spatial resolution is still low due to high scattering of photons. By using NIR contrast agents changes in absorption and/or scattering would be desired such that higher contrasts between tumour and non-diseased tissue result.

One NIR fluorescent dye that has already been used as a contrast agent to detect tumours in animals and humans is indocyanine green (ICG) [9–12]. The

[1] Schering AG, Research Laboratories, Berlin, Germany.
[2] Physikalisch-Technische Bundesanstalt, Berlin, Germany.
[3] Schering AG, Clinical Development Diagnostics and Radiopharmaceuticals, Berlin, Germany.
[4] Chirurgie und chirurgische Onkologie, Charité-Universitätsmedizin Berlin, Campus-Buch.
[5] To whom correspondence should be addressed at Schering AG, Optical Imaging & New Modalities Research, Müllerstrasse, 13342 Berlin, Germany. E-mail: christin.perlitz@schering.de

Abbreviations: CCD, charge-coupled device; MRI, magnetic resonance imaging; NIR, near infrared.

low molecular weight dye ICG is originally used for examination of liver function, non-invasive measurement of cardiac output and fluorescence angiography in ophthalmology [13,14]. It is strongly bound to plasma proteins, shows negligible extravasation and is rapidly taken up by the liver [15,16]. Therefore, plasma levels fall within minutes after i.v. injection to very low levels, thus limiting the time window suitable for optical measurements [17].

The objective of our work is to elucidate the potential of indocyanine-based imaging agents of a simple, non-specific structure by changing the chemical characteristics of the dyes and study the resulting imaging properties. In particular, we report the properties of a novel cyanine dye based on the indotricarbocyanine chromophore as a potential non-targeted contrast agent. This novel tetrasulfonated carbocyanine dye, abbreviated as TSC, is compared to a previously synthesized hydrophilic dye called SIDAG, which has improved properties in comparison to ICG [17].

Both agents are compared concerning their physicochemical and photophysical properties. Furthermore, the *in vivo* imaging properties of both dyes are investigated in a model of tumour bearing mice.

MATERIALS AND METHODS

Synthesis of Dyes

The synthesis of the dye SIDAG has been described previously [17]. The synthesis of the sulfonated dye TSC will be reported elsewhere, which is in principal similar to the synthesis of SIDAG by utilizing structurally modified indolic and glutaconic acid derivatives, respectively, as starting materials [17]. The chemical structure of both dyes is shown in Fig. 1.

Physicochemical and Photophysical Properties

Measurements of plasma protein-binding were performed by ultrafiltration (Amicon Centrifree tubes, cellulose membrane cut-off 30,000) using 400 μL of a 0.5 mg/mL solution of SIDAG or TSC in spiked mouse serum (female NMRI mice). After incubation at 37°C for 1 hr, the tubes were centrifuged for 8 min at 1500g. Absorbance (A) of the solution after incubation was measured before centrifugation and of the filtrate obtained after centrifugation. The free fraction of dye was calculated as ratio of $A_{\text{dye/filtrate}}$ and $A_{\text{dye/before}}$. The plasma protein bound fraction is 100—free fraction (%).

Absorption measurements were performed on a Lambda 2 photometer (Perkin-Elmer GmbH, Überlingen, Germany). Fluorescence properties were measured in PBS with a SPEX Fluorolog fluorometer (Jobin Yvon) (single excitation and emission monochromator, 350 W Xenon lamp, PM Hamamatsu R928) with 2 μM dye solutions. The solutions were excited at 700 nm. Figure 2 shows absorption and fluorescence emission spectra for TSC. For quantum yield measurements the lamp and photomultiplier were calibrated for their spectral sensitivity. The quantum yields obtained are based on ICG in DMSO ($\phi = 0.13$) and NK1967 in DMSO ($\phi = 0.28$) as standards [23].

Animal Model

As a tumour model the fast growing and highly vascularized murine F9-teratocarcinoma was chosen. Figure 3 shows specific immunostaining of tumour blood vessels. An amount of 50 μL of a tumour cell suspension containing 2×10^6 cells were s.c. implanted into the right flank of female nude mice (NMRI/nu/nu, 25 g, Tierzucht und haltung, Schönwalde, Germany). Tumour growth was controlled twice weekly, tumour size was measured using a digital gage. Tumour volume was calculated using the following formula: $V = (a \times b^2)/2$ with a being the length and b the width of the tumour.

Tumour growth was heterogenous. After 7–10 days of tumour implantation, animals were chosen for imaging. At that time tumour volumes varied between 100 and 950 mm^3.

The animal studies were performed following a protocol approved by the Regional Animal Research

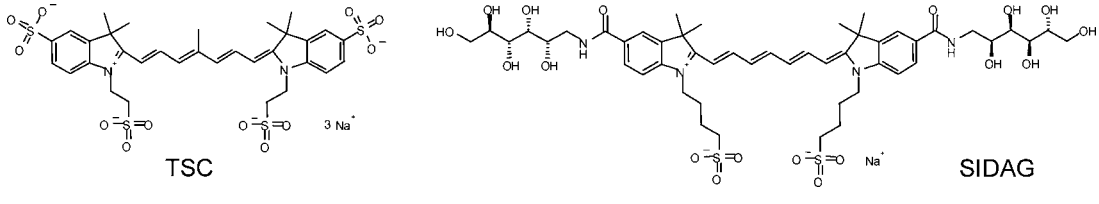

Fig. 1. Chemical structures of investigated low molecular weight cyanine dyes. TSC (MW: 836.9 g/mol) consists of a indotricarbocyanine core with four negatively charged sulfonate groups; SIDAG (MW: 1089.2 g/mol) employs two sulfonate groups and two hydrophilic and neutral glucamide residues.

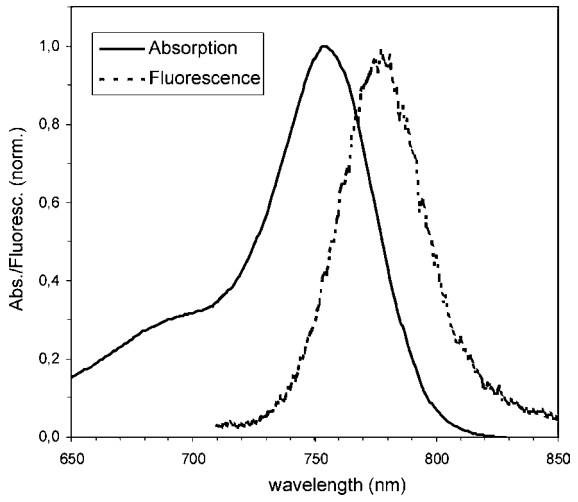

Fig. 2. Absorption and fluorescence spectrum of TSC (in phosphate-buffered saline, pH 7.4). Absorption maximum: 755 nm; fluorescence emission maximum: 778 nm. SIDAG shows similar spectra, for comparison see [17].

Committee (authorized by Landesamt für Arbeitsschutz, Gesundheitsschutz und Technische Sicherheit Berlin No. A 0136/01).

In Vivo Fluorescence Measurements

To reduce autofluorescence of animals caused by standard diet, animals were fed with a manganese-free diet (ssniff R/M-H, ssniff Spezialdiäten GmbH, Soest, Germany) 7–10 days prior to imaging experiments. Animals were injected intravenously with the corresponding dye dissolved in physiological saline at a dose of 2 μmol/kg body weight into the tail vein. Typically for a 20 g animal a volume of 200 μL was injected. For each measurement the animals were anesthetized. A short-time anesthesia was induced using the inhalation anesthetics isoflurane (Isofluran Curamed, Curamed Pharma GmbH, Karlsruhe, Germany).

The imaging device is shown in Fig. 4 comprising the following units: a continuous wave diode-laser with a maximum power of 1.5 W (Type Ceralas PDT 742 nm /1.5 W, Ceram Optec GmbH, Bonn, Germany), a high resolution (1344 pixel $\times$ 1024 pixel) Peltier cooled CCD-Camera (Type C4542-95-12ER, Hamamatsu), a glass fibre for excitation (Type 613-831-0981, OZ Optics Ltd, 5 m length) and a light-dense measurement cabin (1000 mm height, 600 mm width and 400 mm depth). For excitation two band pass filters at once, a (740.0 ± 2.5) nm, ($T_{max} > 70\%$) and a LCS 740-F with (740 ± 2) nm, ($T_{max} > 50\%$) were used. To cut off scattered excitation light two band pass filters (802.5 ± 5.0) nm, ($T_{max} > 80\%$) and (801 ± 3) nm, ($T_{max} > 70\%$) were used. The fluorescence was imaged using the cooled CCD-camera with an objective (Type XNP 1.4/23-0302 CM120, Schneider, Optische Werke GmbH, Kreuznach, Germany).

Imaging Procedure

After intravenous application of the respective dye into tumour-bearing nude mice the dye was excited by

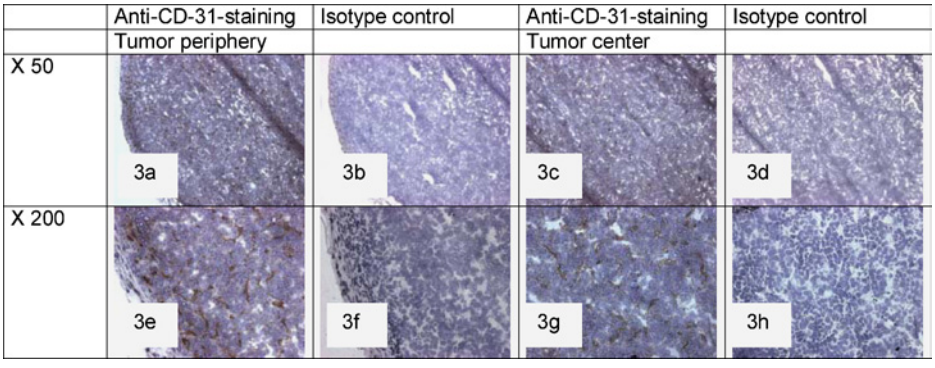

Fig. 3. Immunohistochemistry staining of vascular endothelial cells in a murine F9-teratocarcinoma of 600 mm^3 tumour volume, original magnifications 50$\times$ and 200$\times$. Cryoconserved F9-teratocarcinoma were cut into slices and mounted on microscope slides. Using immunohistochemical staining blood vessels are visualized using an antibody directed against vascular endothelial cells (anti-CD31-stain) yielding a brown colour where blood vessels are located in the tumour tissue. In the isotype control staining the primary antibody (rat anti-mouse-CD) is replaced by an antibody consisting of the same rat immunoglobuline class but no specificity for a mouse protein. Thus, no brown staining should occur using the isotype antibody. Anti-CD31-staining results in decoration of blood vessels in the tumour periphery and center of F9-teratocarcinoma (e and g) whereas no staining is visible in the isotype controls of tumour periphery and center (f and h). This is proof that the brown colour results from a specific binding of the antibody to vascular endothelial cells.

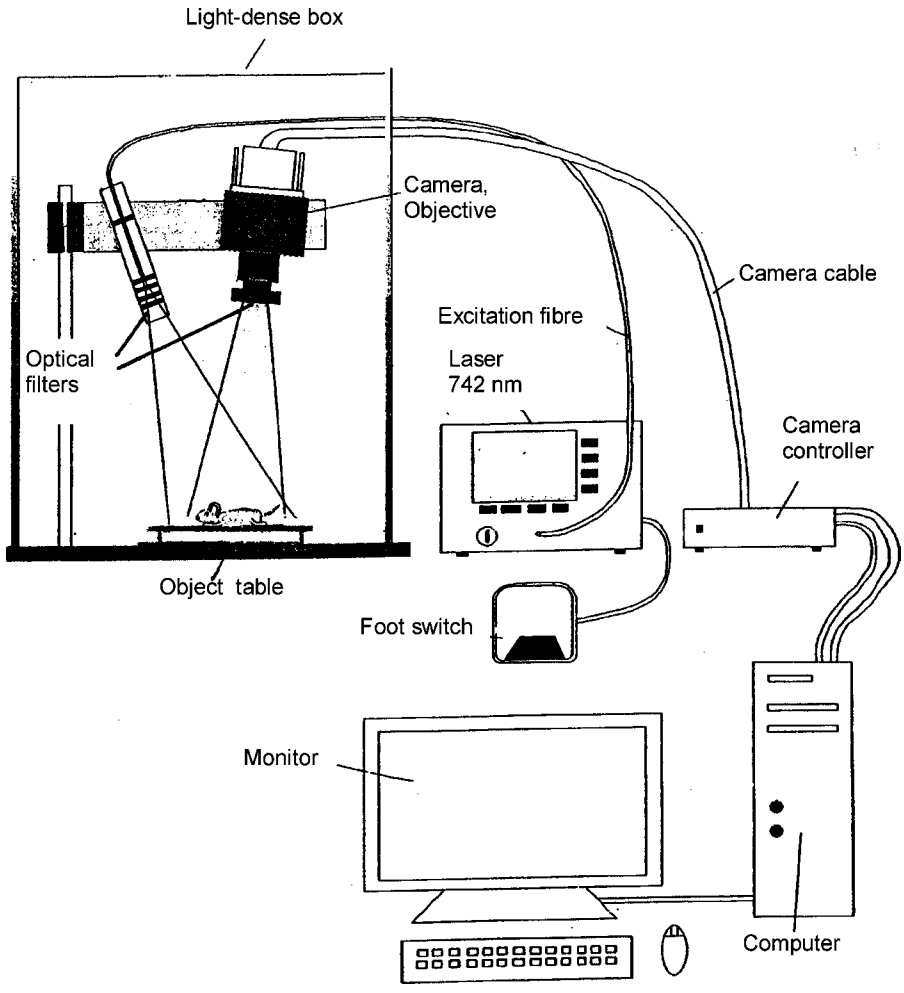

Fig. 4. Schematic drawing of the imaging device. The laser emitting light of 742 nm is connected to a laser fibre that ends in a light dense imaging box at a fixed position. The measurement cabin has a size of approximately 1000 mm (height) × 600 mm (width) × 400 mm (depth). The animal is positioned on the object table inside the measurement cabin. The reflected fluorescence from the animal is detected with a camera. Via a camera cable and camera controller there is a connection to the computer and monitor to visualize the reflected fluorescence. For more details see Materials and Methods.

the laser light and detected using the cooled CCD-camera (capture resolution 672 pixel × 512 pixel). The emitted fluorescence was imaged at different times after application of dyes until 48 hr. The animals were horizontally positioned on a black neoprene-mat at the bottom of the measurement cabin, which was inside coloured in black. Furthermore, the black mat at the bottom of the measurement cabin (Betech GmbH, Berlin, Germany) was used to reduce reflectance of excitation light.

First, an image prior to dye application was taken for every animal, using a standard power of 10 mW/cm^2 and an exposure time of 4.0 s. After intravenous application of the dye images were taken at the following points in time: 1, 10 and 30 min; 1, 4, 7, 24 and 48 hr after i.v. injection. Then, imaging parameters such as exposure time and laser power were chosen in such a way, that the full dynamic range of the camera could be exploited. Images without illumination were taken with different exposure times to subtract the electronic background from all pictures using the respective background image.

Data Processing and Image Analysis

Fluorescence images were stored on a hard disk and analysed using the PCI-Software (Compix Inc., Imaging Systems, Hamamatsu). Tumour tissue and non-diseased

tissue as a control region were chosen as regions of interest. As the control region an observer optimized region contralateral to the tumour region was determined. Manually, the regions of interest were marked in each picture. Then, for both the tumour regions and the control regions the fluorescence intensities were quantified using the special software NIR-XP developed at Schering AG, Berlin. As a representative value of fluorescence the 90th percentile of the grey-scale population per region of interest was chosen. Finally, for all imaging points in time the fluorescence intensities of tumours were compared with control regions.

RESULTS

Photophysical and Physicochemical Properties

Both dyes are based on the indotricarbocyanine chromophore bearing sulfonated alkyl chains at the indolic nitrogens and substituents at the exterior ring positions. While the previously described SIDAG [15] is a disulfonated derivative with two glucamine residues, the structure of TSC contains four sulfonate groups rendering the molecule a compact, tri-anionic molecule and an additional methyl group at the polymethine chain. Both compounds are almost identical in their absorption and fluorescence emission spectra [15], while the fluorescence quantum yield of TSC is improved in aqueous media (10% for TSC and 6.5% for SIDAG).

While SIDAG has a free fraction of 40%, the measured free fraction of TSC is lower (26%) corresponding to an increased plasma protein binding of 74% for the plasma species used. The reported value of 10% plasma protein binding for SIDAG [15] obtained by equilibrium dialysis is not directly comparable as both a different method and a different calculation was applied. The plasma protein binding of SIDAG was in the earlier publication [15] defined as a substraction, but corresponds well to the results described herein when re-calculating the raw data with the formula applied here (gives 43% free fraction).

Fluorescence Imaging

The performance of the newly synthesized dye TSC as a contrast agent for fluorescence imaging was evaluated in a syngenic subcutaneously implanted tumour in nude mice in comparison to the dye SIDAG. Fluorescence images were taken until 48 hr after i.v. injection. For the fluorescence images the brightness of background was varied such that for all measurements, even before application of the fluorescent substance, the mouse becomes visible (Figs. 5a and b). This procedure generates fluorescence images that show only relative fluorescence intensities within one single picture. Values permitting a semi-quantitative comparison of signal emission from different regions in the animals over time were received by determining fluorescence intensities (counts) for the regions of interest, tumour versus non-diseased tissue, respectively (Figs. 6a–d and 7).

For each dye a representative sequence of fluorescence images after intravenous application in one investigated animal is presented in Figs. 5a and b. All pictures are inverse images. By visual inspection of these images a clear discrimination between tumour and non-diseased tissue was possible for TSC 4 and 7 hr after i.v. application. For SIDAG a discrimination between tumour and non-diseased tissue was possible starting at 4 hr after injection and maintained until 48 hr. For SIDAG also a strong fluorescence from both kidneys could be detected at 4 and 7 hr after application.

Looking at the fluorescence intensities (FI) in dependence on observation time, both dyes reached a maximum FI in the tumour region already 10 min after i.v. application. In our experimental setting, this value was 800,000 counts for TSC and roughly a million counts for SIDAG. At that time FI in the control regions were even a little higher with 950,000 counts for TSC and approximately 1,100,000 for SIDAG (see Fig. 7 insert). Until 4 hr after application, both dyes showed similar decrease of FI in both tumour and control regions. At 4 hr after application for both dyes the FI were below 100,000 counts with higher values in the tumour compared to the control region. The main differences for both dyes became apparent from 4 hr and later measurements. Whereas TSC showed a strong decrease in FI between 4 and 7 hr after application for both tumour and control region, the decrease was much less for SIDAG. This difference was even more pronounced at 24 and 48 hr, when there was hardly any fluorescence detectable with TSC. In turn, SIDAG yielded still high values in the tumours, which allowed a robust visible discrimination of the tumour from its surrounding area. FI over time are given in Figs. 6a–d for the different regions of interest (tumour vs. control region) and for individual animals of different groups (TSC vs. SIDAG). Figure 7 represents FI values as geometric means of the two investigated contrast agents, for both the control and tumour regions. Finally, the resulting contrasts were calculated and are illustrated in Fig. 8 clearly demonstrating the different behaviour of both dyes in particular towards longer observation times.

DISCUSSION

The experimental study presented here was conducted to investigate two unspecific near infrared dyes

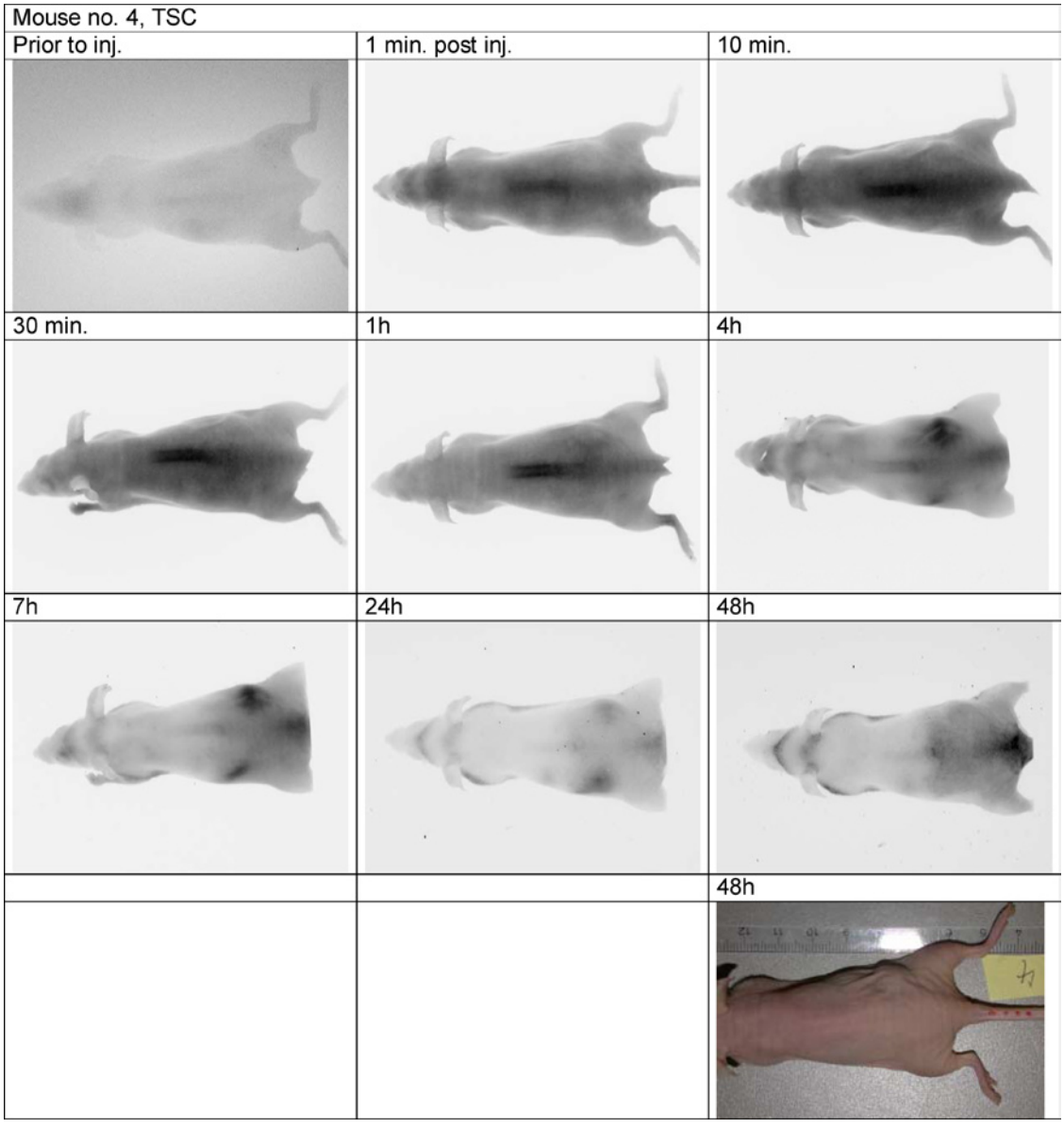

Fig. 5. Exemplary fluorescence images of one animal for each contrast agent after injection of 2 μmol/kg dye intravenously into F9-teratocarcinoma bearing mice after injection of TSC (a). Here, the tumour can be clearly seen at the right body side close to the right flank 4 and 7 hr after injection. Fluorescence on the left body side opposite of the tumour, because of its specific localisation, probably represents dye uptake into the spleen. Injection of SIDAG (b): the tumour can be clearly visualized at the right body side close to the right flank 4, 7, 24 and 48 hr after injection. In some pictures little black spots on the animals feet may be visible because of contaminations on the mouse skin resulting from urination of the animals.

with respect to their pharmacokinetic behaviour and imaging properties in an experimental tumour model.

The widely used MRI and some X-ray contrast agents, which are, applied intravenously are considered as extracellular-agents because they extravasate into the extracellular fluid. Slow extravasation is often caused by the ability to bind to plasma proteins [18,19]. The optical agents described here are intended to follow this behaviour. However, the exact mode of action for the investigated NIR-dyes is still unclear. When administered intravenously, the dye ICG has a plasma half-life of 2–4 min [20,21], which can be explained by a fast uptake into the liver. Its specific accumulation in tumour tissue compared to non-diseased tissue, as described in *in vivo*

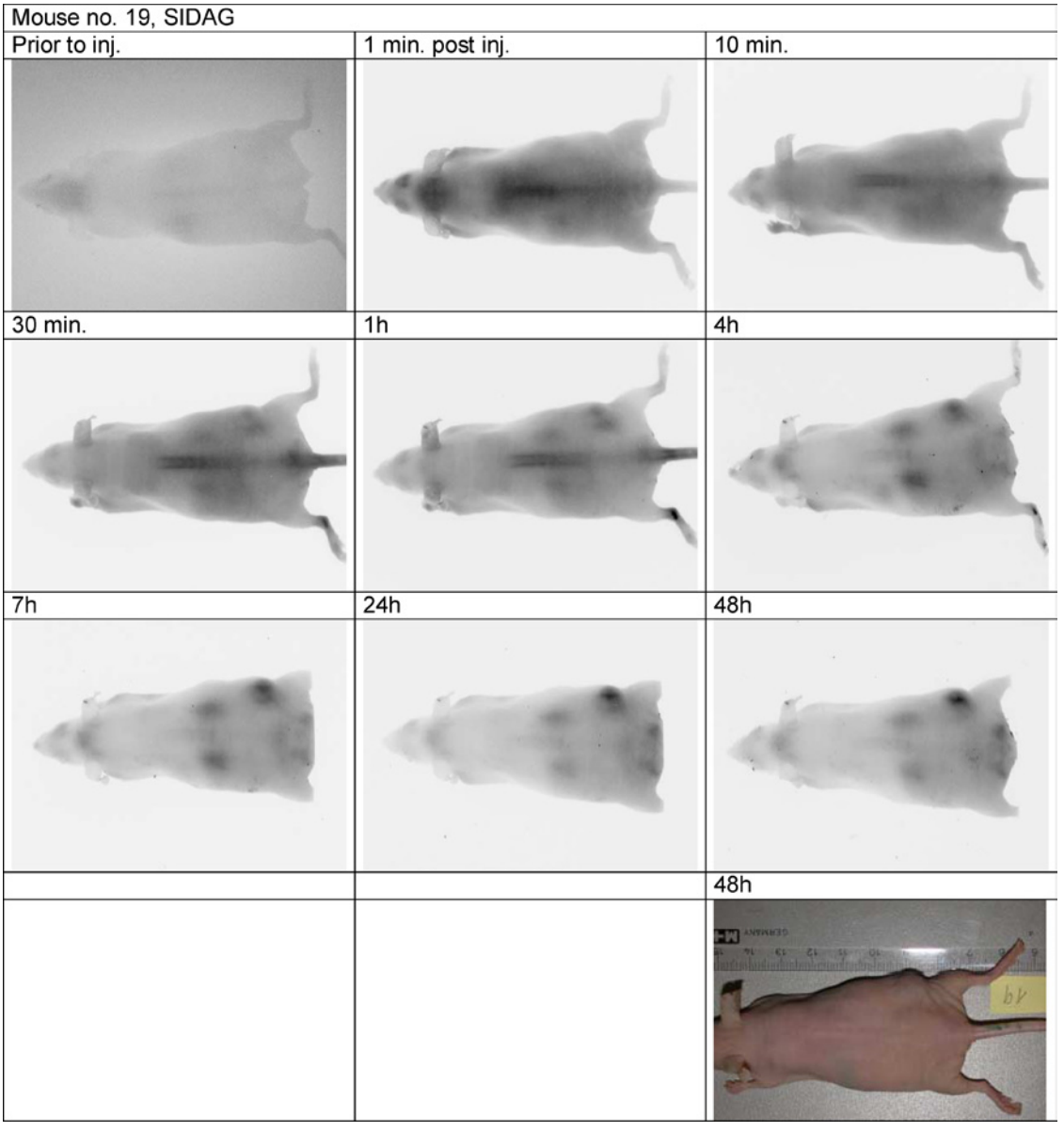

Fig. 5. Continued.

experiments [22,23], is so far thought to be explained by an extravasation of the NIR-dyes through fenestrated tumour blood vessels. Because of the extensive protein binding and the early liver uptake of ICG the amount of extravasation is rather low and yields a fluorescence contrast only at early points in time after application. This results, i.e. in a maximum contrast between tumour and normal tissue of 1.6% 10 min after i.v. injection in a 9 L glioma grafted s.c. into rats [15].

Comparable to ICG, our newly synthesized dye TSC shows a rather high protein binding in plasma, although the chemical modification by sulfonic acid groups made us expecting a much lower plasma protein binding. Nonetheless, the pharmacokinetics in tumour bearing animals is still different. The fluorescence intensities over time show high values soon after i.v. injection for the tumour and control region peaking at 10 min. Furthermore, the net fluorescence, resulting from the ratio between tumour and control region, rises rather slowly after application, reaching its maximum 7 hr after i.v. application. Because of this, we can hypothesize, that no fast liver uptake comparable to ICG occurs, which might be caused by the

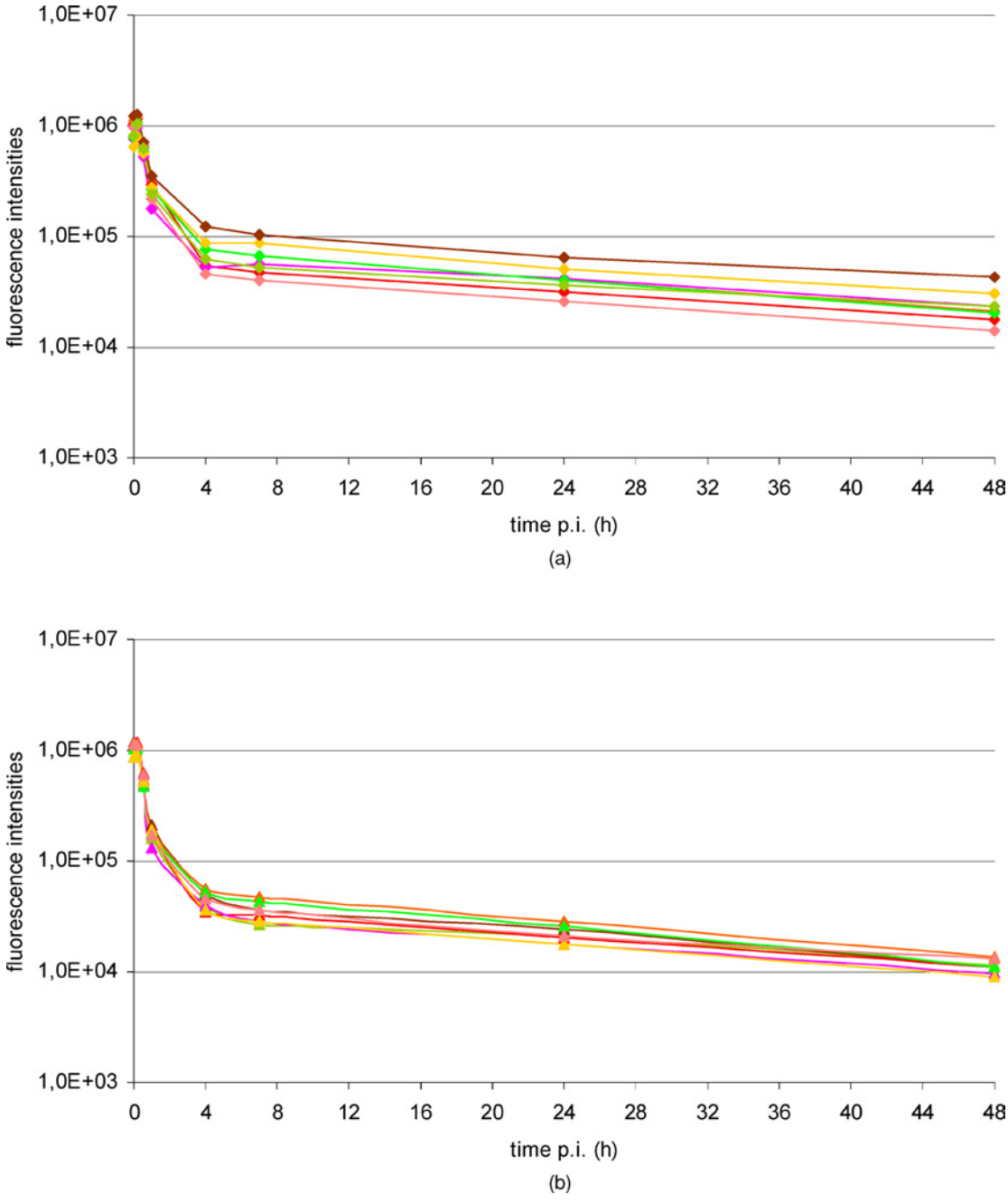

Fig. 6. Fluorescence intensities versus time after injection of 2 μmol/kg dye intravenously into F9-teratocarcinoma bearing mice. Fluorescence intensities are given for each animal in logarithmic scale to show individual variations. Fluorescence intensities in tumour regions of eight investigated animals after injection of SIDAG (a), fluorescence intensities in control regions of the same eight investigated animals after injection of SIDAG (b), fluorescence intensities in tumour regions of nine investigated animals after injection of TSC (c), and fluorescence intensities in control regions of the same nine investigated animals after injection of TSC (d). All values are corrected for electronic background fluorescence. Electronic background fluorescence is the calculated fluorescence without illumination for different exposure times which results in visible fluorescence on the camera picture. This electronic background fluorescence is then subtracted from the calculated fluorescence in the different regions, tumour and control tissue for every animal and every time point of measurement.

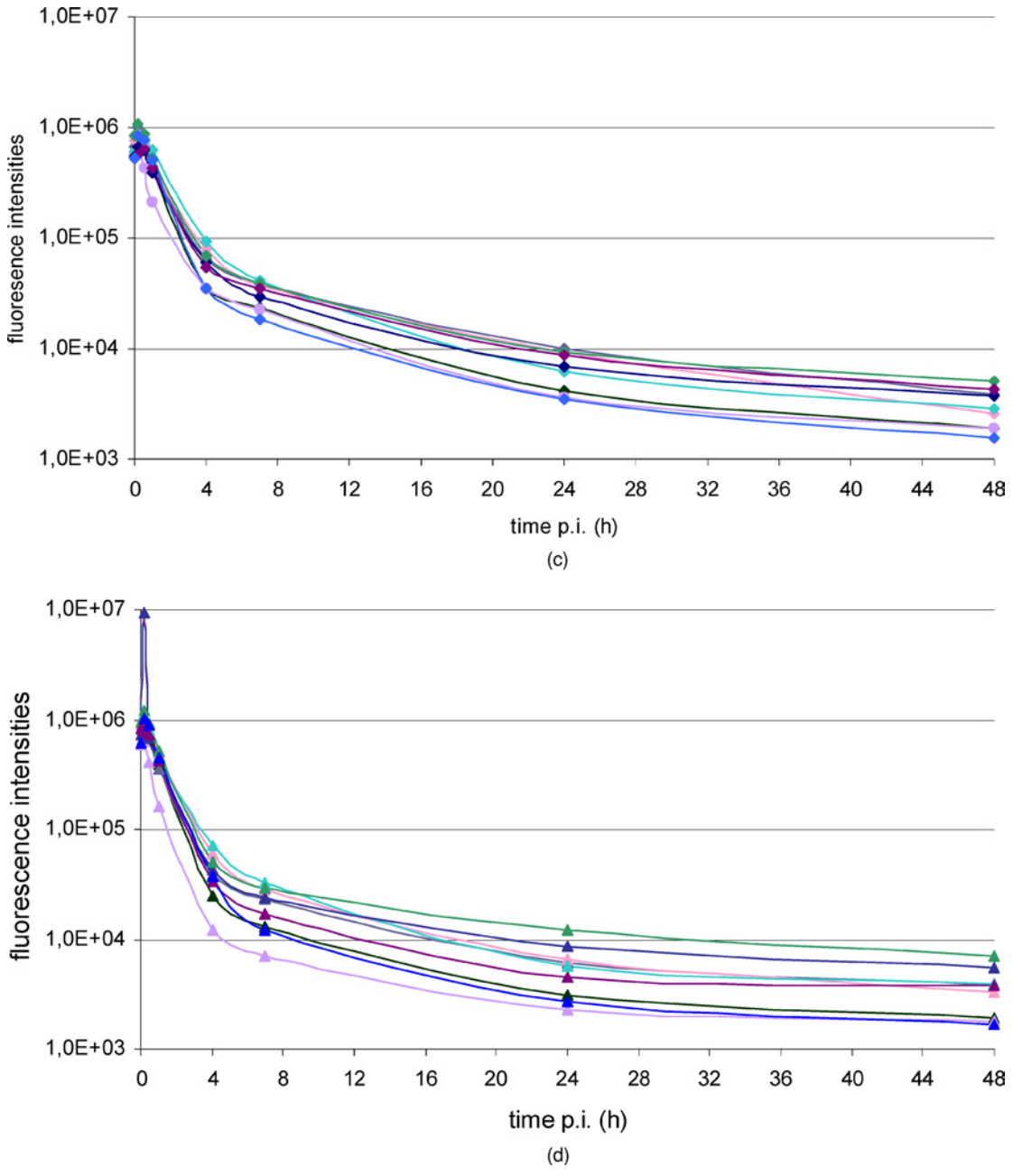

Fig. 6. Continued.

enhanced free fraction of non-bound dye molecules. The previously synthesized dye SIDAG has different properties in terms of increased hydrophilicity, which leads to a reduced protein binding ability. Looking at pharmacokinetics this leads to a fast increase of net fluorescence. One hour after application there is a significantly higher FI in the tumour region compared to the control region and this difference is still increasing until the last point of measurement 48 hr post injection.

Regarding the FI for both dyes 10 min after application, the values are very similar, being around 800,000 to 1 million FI, showing slightly elevated values for the control regions, which can be attributed to the often postulated higher interstitial blood pressure in tumours that aggravates uptake of molecules into this tissue [22]. Over time both dyes then show a very similar behaviour in terms of decreasing FI up to 4 hr. Later on, there are major pharmacokinetic differences. For TSC the decline of FI

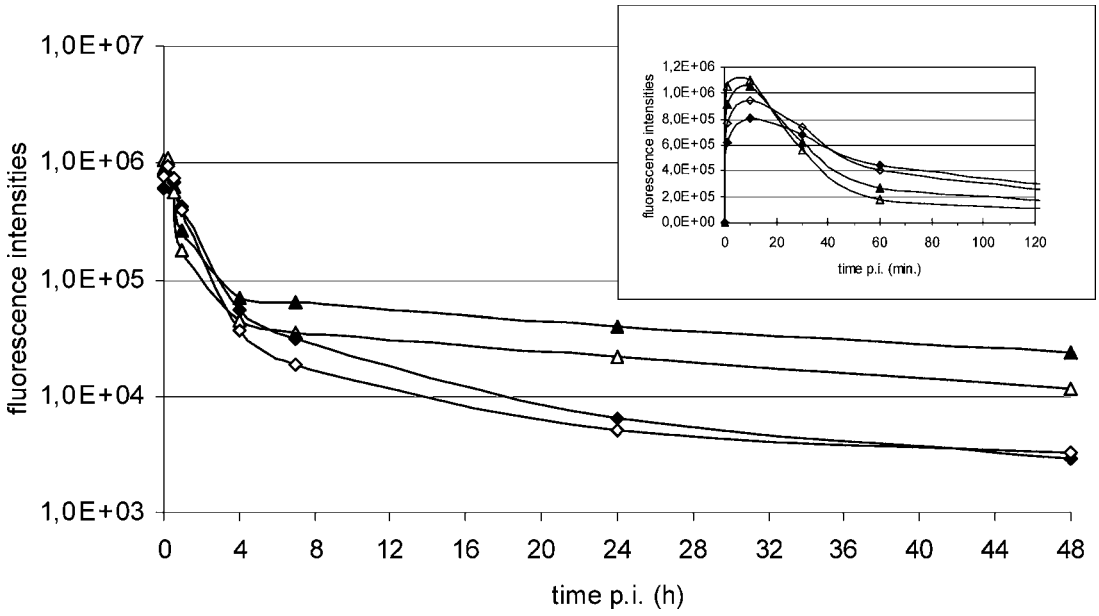

Fig. 7. Average fluorescence intensities (geometric mean of measured values) versus time after injection of 2 μmol/kg dye intravenously into F9-teratocarcinoma bearing mice (SIDAG $n = 8$, TSC $n = 9$). Insert: Data extract from this figure including data points up to 1 hr observation time. Fluorescence intensities in tumour and control regions after injection of SIDAG; open triangles represent control regions, closed triangles represent tumour regions. Fluorescence intensities in tumour and control regions after injection of TSC; open squares represent control regions, closed squares represent tumour regions. All values are corrected for electronic background fluorescence.

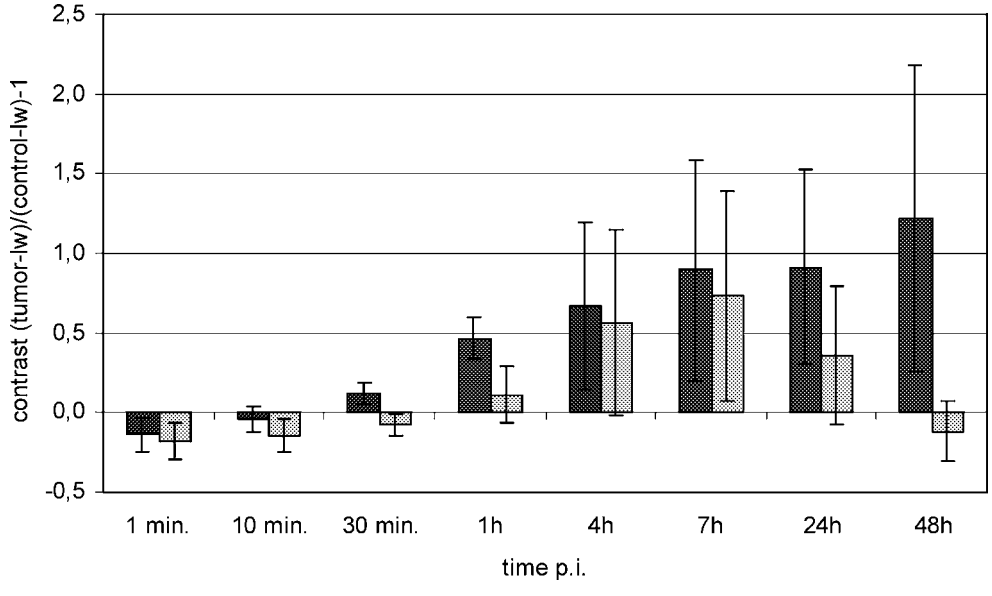

Fig. 8. Average fluorescence contrast between tumour and control regions for both contrast agents with observation time. Contrast between both tissues was calculated as fluorescence intensities in the tumour after dye application minus fluorescence intensities in the tumour before dye application divided by the corresponding values in the control region. From this ratio the value of one is then subtracted, resulting in positive values for fluorescence accumulation in the tumour region and negative values for fluorescence accumulation in the control region. Values for SIDAG are given in black ($n = 8$), values for TSC are given in grey ($n = 9$).

in tumour and control region continues steadily, resulting in a visible contrast not later than 7 hr after application. On the other hand for SIDAG the FI decline is delayed, resulting in tumour demarcation from the surrounding tissue until 48 hr after i.v. application. At that time FI in the tumour regions were still 2.5% of the maximum measured FI 10 min after application and 1% for the control regions, respectively. For TSC the FI in both tumour and control regions are very similar at the latest measurement and correspond to approximately 0.3% of the maximum measured FI also 10 min after application.

The prominent fluorescence of SIDAG in the kidneys 4 and 7 hr after application suggests a renal uptake. Since the differences in fluorescence intensities between tumour and control regions stay almost the same until the last measuring point at 48 hr, it can be hypothesized that by tubular reabsorption a certain amount of dye reenters the circulation and leads to prolonged contrasts between tumour and control tissue. From our own unpublished data we know that for SIDAG in rats two-thirds of elimination is via urine. On the basis of the assumption of a two-compartment model the renal elimination half-life time is 220 min.

For TSC no fluorescence in the kidneys was observed. After i.v. application of comparable amounts of TSC excretion is almost complete after 1–2 days in rats and dogs. In dogs excretion occurs mostly (72–88%) via urine, in rats excretion occurs mostly (70%) in feces (data not shown).

In conclusion we have presented *in vivo* imaging data of two non-targeted contrast agents with a structural similarity to ICG but still distinct structural differences leading to different features regarding protein binding, pharmakokinetics and excretion pathways. TSC showed a delayed fluorescence increase and rapid clearance from the tumour resulting in a diagnostic window between 4 and 7 hr after injection. SIDAG showed a faster fluorescence increase and delayed clearance from the tumour resulting in a diagnostic window between 4 and 48 hr after injection.

For the use in *in vivo* imaging settings both dyes are potent contrast agents leading to a discrimination of tumour and control regions in the presented s.c. tumour model. Because of differences in background intensities between the fluorescence images of different animal individuals, slight changes in fluorescence intensities are rather difficult to determine precisely. A more quantitative evaluation is desirable, e.g. by acquiring fluorescence intensities obtained from a defined reference area chosen within the animal or better by well characterized and preferably certified fluorescence standards of liquid or solid nature with known thermal and photochemical stability.

ACKNOWLEDGMENTS

We thank Astrid Knop and Stefan Wisniewski for their excellent technical assistance.

REFERENCES

1. E. E. Graves, R. Weissleder, and V. Ntziachristos (2004). Fluorescence molecular imaging of small animal tumor models. *Curr. Mol. Med.* **4**, 419–430.
2. J. P. Houston, A. B. Thomson, M. Gurfinkel, and E. M. Sevick-Muraca (2003). Sensitivity and depth penetration of continuous wave versus frequency-domain photon migration near-infrared fluorscence contrast-enhanced imaging. *Photochem. Photobiol.* **77**, 420–430.
3. B. Ebert, U. Sukowski, D. Grosenick, H. Wabnitz, K. T. Moesta, K. Licha, A. Becker, W. Semmler, P. M. Schlag, and H. Rinneberg (2001). Near-infrared fluorescent dyes for enhanced contrast in optical mammography: Phantom experiments. *J. Biomed. Opt.* **6**, 134–140.
4. M. A. Francescini, K. T. Moesta, S. Fantini, G. Gaida, E. Gratton, H. Jess, W. W. Mantulin, M. Seeber, P. M. Schlag, and M. Kaschke (1997). Frequency-domain techniques enhance optical mammography: Initial clinical results. *Proc. Natl. Acad. Sci. USA* **94**, 6468–6473.
5. L. Goetz, H. Heywang-Koebrunner, O. Schuetz, and H. Siebold (1998). Optische Mammographie an praeoperativen Patientinnen. *Acad. Radiol.* **8**, 31–33.
6. D. Grosenick, H. Wabnitz, H. Rinneberg, K. T. Moesta, and P. M. Schlag (1999). Development of a time-domain optical mammograph and first in vivo applications. *Appl. Opt.* **38**, 2927–2943.
7. D. Grosenick, K. T. Moesta, H. Wabnitz, J. Mucke, Ch. Stroszynski, R. MacDonald, P. M. Schlag, and H. Rinneberg (2003). Time-domain optical mammography: Initial clinical results on detection and characterization of breast tumors. *Appl. Opt.* **42**, 3170–3186.
8. V. Ntziachristos and R. Weissleder (2002). Charge-coupled-device based scanner for tomography of fluorescent near-infrared probes in turbid media. *Med. Phys.* **29**(5), 803–809.
9. X. Li, B. Beauvoit, R. White, S. Nioka, B. Chance, and G. Yodh (1995). Tumor localization using fluorescence of indocyanin green (ICG) in rat models. *SPIE* **2389**, 789–798.
10. J. S. Reynolds, T. L. Troy, R. H. Mayer, A. B. Thompson, D. J. Waters, K. K. Cornell, P. W. Snyder, and E. M. Sevick-Muraca (1999). Imaging of spontaneous canine mammary tumors using fluorescent contrast agents. *Photochem. Photobiol.* **70**, 87–94.
11. S. Zhao, M. A. O'Leary, S. Nioka, and B. Chance (1995). Breast tumor detection using continuous wave light source. *SPIE* **2389**, 789–798.
12. M. M. Haglund, M. S. Berger, and D. W. Hochmann (1996). Enhanced optical imaging of human gliomas and tumor margins. *Neurosurgery* **38**, 309–317.
13. C. M. Leevy, F. Smith, J. Longuevill, G. Paumgartner, and M. M. Howard (1967). Indocyanine green clearance as a test for hepatic function. Evaluation by dichromatic ear densitometry. *J. Am. Med. Assoc.* **200**, 236.
14. R. W. Flower and B. E. Hochheimer (1976). Indocyanine green dye fluorescence and infrared absorption choroidal angiography performing simultaneously with fluorescein angiography. *John Hopkins Med. J.* **138**, 33–42.
15. G. Paumgarten, P. Probst, K. Kraines, and C. M. Leevy (1970). Kinetics of indocyanine green removal from the blood. *N. Y. Acad. Sci.* **170**, 134–114.
16. D. K. F. Meijer, B. Weert, and G. A. Vermeer (1988). Pharmakokinetics of biliary excretion in man. VI. Indocyanine green. *Eur. J. Clin. Pharmacol.* **35**, 295–303.

17. K. Licha, B. Riefke, V. Ntziachristos, A. Becker, B. Chance, and W. Semmler (2000). Hydrophilic cyanine dyes as contrast agents for near-infrared tumor imaging: Synthesis, photophysical properties and spectroscopic *in vivo* characterization. *Photochem. Photobiol.* **72**, 392–398.
18. P. Dawson (1996). X-ray contrast-enhancing agents. *Eur. J. Radiol.* **23**, 172–177.
19. A. N. Oksendal and P.-A. Hals (1993). Biodistribution and toxicity of MR imaging contrast media. *JMRI* **1**, 157–165.
20. S. Mordon, J. M. Devoiselle, S. Soulie-Begu, and T. Desmettre (1998). Indocyanine green: Physisochemical factors affecting its fluorescence in vivo. *Microvasc. Res.* **55**, 146–152.
21. T. Desmettre, J. M. Devoiselle, and S. Mordon (2000). Fluorescence properties and metabolic features of indocyanine green (ICG) as related to angiography. *Surv. Opthalmol.* **45**, 15–27.
22. X. Intes, J. Ripoll, Y. Chen, S. Nioka, A. G. Yodh, and B. Chance (2003). *In vivo* continuous-wave optical breast imaging enhanced with indocyanine green. *Med. Phys.* **30**, 1039–1047.
23. V. Ntziachristos, A. G. Yodh, M. Schnall, and B. Chance (2000). Concurent MRI and diffuse optical tomography of breast after indocyanine green enhancement. *PNAS* **97**, 2767–2772.
24. J. R. Less, M. C. Posner, Y. Boucher, D. Borochovitz, N. Wolmark, and R. K. Jain (1992). Interstitial hypertension in human breast and colorectals tumors. *Cancer Res.* **52**, 6371–6374.